

# Evidence for crossed Andreev reflections in bilayers of (100) YBa<sub>2</sub>Cu<sub>3</sub>O<sub>7- $\delta$</sub> and the itinerant ferromagnet SrRuO<sub>3</sub>

Itay Asulin,<sup>1</sup> Ofer Yuli,<sup>1</sup> Gad Koren,<sup>2</sup> and Oded Millo<sup>1,\*</sup>

<sup>1</sup>*Racah Institute of Physics, The Hebrew University of Jerusalem, Jerusalem 91904, Israel*

<sup>2</sup>*Department of Physics, Technion-Israel Institute of Technology, Haifa 32000, Israel*

(Received 23 July 2006; published 1 September 2006)

Scanning tunneling spectroscopy measurements on thin epitaxial SrRuO<sub>3</sub>/(100)YBa<sub>2</sub>Cu<sub>3</sub>O<sub>7- $\delta$</sub>  ferromagnet/superconductor bilayers, reveal localized regions in which the superconductor order parameter penetrates the ferromagnet to more than 26 nm, an order of magnitude larger than the coherence length in the ferromagnetic layer. These regions consist of narrow (<10 nm) and long strips, separated by at least 200 nm, consistent with the known magnetic domain wall structure in SrRuO<sub>3</sub>. This behavior may be due to crossed Andreev reflections, taking place in the vicinity of the magnetic domain walls.

DOI: [10.1103/PhysRevB.74.092501](https://doi.org/10.1103/PhysRevB.74.092501)

PACS number(s): 74.45.+c, 74.50.+r, 74.81.-g

In spite of the considerable research over the past few years, a comprehensive understanding of the proximity effect (PE) in superconductor (*S*) ferromagnet (*F*) heterostructures has not yet been established. Such systems are of interest since they allow a direct investigation of the interplay between the two competing orders of superconductivity and magnetism. In an *N/S* proximity system, where *N* is a normal metal in good electrical contact with *S*, superconducting correlations are induced in *N* over a length scale of the normal coherence length  $\xi_N$ , while they are weakened in the *S* side over a scale of the superconducting coherence length  $\xi_S$ .<sup>1</sup> The mechanism underlying the PE at *S/N* interfaces is the Andreev reflection (AR). Upon impinging on the interface from the *N* side, holelike quasiparticles are retro-reflected as electronlike quasiparticles with inverse spin (maintaining phase coherence over  $\xi_N = \sqrt{\hbar D/k_B T}$  where *D* is the diffusion coefficient), while destroying Cooper pairs in the *S* side. Consequently, the PE is expected to be significantly suppressed when the *N* side is replaced by a ferromagnet due to spin polarization.<sup>2</sup> Theoretical works based on the Fulde, Ferrell, Larkin, and Ovchinnikov (FFLO) mechanism,<sup>3,4</sup> predict a rapid and nonmonotonic decay of the superconducting order parameter (OP) in *F*, of the form  $\sin(x/\xi_F)/(x/\xi_F)$  in the clean limit and  $\exp(-x/\xi_F)\cos(x/\xi_F)$  in the dirty limit (where *x* is the distance from the interface).<sup>5,6</sup> The corresponding coherence lengths in *F* where the exchange energy is  $E_{\text{ex}}$ , are  $\xi_F = \hbar v_F/2E_{\text{ex}}$  (clean limit), and  $\xi_F = \sqrt{(\hbar D/2E_{\text{ex}})}$  (dirty limit), which are typically of the order of a few nm, much shorter than  $\xi_N$ . For certain thicknesses of the *F* layer a “ $\pi$  state” may appear, in which the induced OP in *F* reverses its sign.<sup>5,6</sup>

Many studies confirmed these predictions and clearly demonstrated damped OP oscillations in *F* and a corresponding dependence on the *F* thickness of the critical current in *SFS* junctions.<sup>7,8</sup> All of these effects occur on a length scale of a few nm, in agreement with estimates for  $\xi_F$ . However, other experiments show a long range PE where the penetration depth of the induced order parameter in *F* is two orders of magnitude larger than  $\xi_F$ .<sup>9,10</sup>

The predictions concerning the *S/F* proximity systems result from the singlet pairing in *S*, and are independent of the

symmetry (*s* or *d* wave) of the order parameter.<sup>11,12</sup> However, the anisotropy of the *d*-wave symmetry is expected to manifest itself in the PE (Ref. 11) (as in the case of Au/YBCO bilayers we have previously studied<sup>13,14</sup>), in the phase, amplitude and period of the oscillations in *F*. Here too, experiments provide contradictory results. While Ref. 15 reports short range damped oscillations in *F*, data measured on *SFS* Josephson junctions indicate a long range PE, sustaining for *F* thickness of up to 40 nm.<sup>16–20</sup>

One possible explanation for the long range PE is given by the formation of a strong triplet pairing amplitude component.<sup>21,22</sup> Alternately,<sup>16,23</sup> superconducting correlations can penetrate *F* to a distance much longer than  $\xi_F$  in the vicinity of magnetic domain walls (DW) at the *S/F* interface via the crossed Andreev reflection (CARE) effect. This process was first discussed for two spatially separated *N/S* junctions,<sup>24</sup> and then for three terminal *S/F* hybrids.<sup>25</sup> Here, a spin-polarized hole arriving from one magnetic domain is Andreev reflected as an electron in an adjacent domain having opposite spin polarization. In order for CARE to occur, the width of the DW must be within a few  $\xi_S$ .<sup>24,25</sup> Peña *et al.*<sup>16</sup> conjectured that CARE can explain their long range PE results in *SF* multilayers, in spite of the fact that the DW width in their case is  $\times 10$  larger than  $\xi_S$ . Recently, evidence for CARE was provided by magnetotransport measurements performed on mesoscopic *S/F* structures consisting of conventional and unconventional superconductors.<sup>26–28</sup> However, a microscopic local-probe observation of this phenomenon and its effect on the density of states (DOS) in the *F* side of the junctions are still lacking.

In this study we employ scanning tunneling spectroscopy on thin epitaxial SrRuO<sub>3</sub>/(100)YBa<sub>2</sub>Cu<sub>3</sub>O<sub>7- $\delta$</sub>  (SRO/YBCO) *F/S* bilayers with various SRO thicknesses. Our measurements show that the OP (induced superconductorlike gap structure) penetrates the SRO to a distance larger than  $10\xi_F$  but only along well defined localized lines which correlate with the underlying magnetic DW structure. This localized long range PE may be accounted for by the CARE process taking place along the DWs of the SRO at the SRO/YBCO interface.

SRO is an itinerant ferromagnet, which is ideally suited for studying the PE with YBCO, in particular the role of the

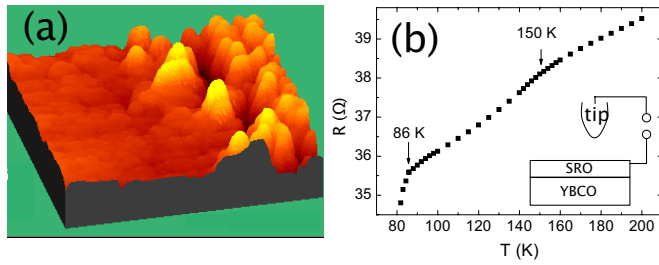


FIG. 1. (Color online) (a) 3D STM topographic image ( $0.45 \times 0.45 \mu\text{m}^2$ ) of a 13 nm thick SRO layer on a 66 nm thick (100)YBCO film showing flat and crystalline regions typical of the bare underlying YBCO film. (b) Resistance vs temperature curve of a 26 nm thick SRO/(100)YBCO bilayer showing both the ferromagnetic transition at  $\sim 150$  K and the onset of the superconducting transitions at 86 K. Inset: experimental setup.

DWs. The lattice parameters of SRO are similar to those of YBCO,<sup>29</sup> and therefore they can form epitaxial heterostructures with highly transparent interfaces, essential for the existence of AR and the PE. The DWs in SRO are  $\sim 3$  nm wide, which is comparable to the YBCO coherence length of  $\xi_S \sim 2$  nm, thus allowing the CARE process to occur. Marshall *et al.*<sup>30</sup> have shown that, depending on the growth orientation on SrTiO<sub>3</sub> substrates, the DW spacing varies between 200 nm and 1  $\mu\text{m}$ . We estimate the value of  $\xi_F$  in SRO to range between 1 nm in the dirty limit and 3 nm in the clean limit.

A total of 12 bilayers of SRO (4 to 26 nm thick) on (100)YBCO (66 nm) were prepared and measured. The (100)YBCO films were prepared by laser ablation deposition on (100)SrTiO<sub>3</sub> wafers in two steps. First, a 22 nm thick template layer of YBCO was deposited at a wafer temperature of 600 °C. Then, a second 44 nm thick YBCO layer was prepared at 760 °C. This produced films with two coexisting *a*-axis phases on about 95% of the film's area (verified by x-ray diffraction). One phase consists of small crystallites, a few unit cells in height ( $\sim 2$  nm), while the other is composed of large areas, atomically smooth on scales of 100 nm (see Ref. 31). The bare YBCO films showed transition temperatures at around 88 K with a transition width of about 2 K, implying nearly optimally doped homogeneous films. Tunneling spectra obtained on the smooth regions of the bare YBCO sample featured 16–18 mV gaps, mainly U shaped, further verifying the *a*-axis orientation.<sup>31</sup> The SRO layer was deposited *in situ* on the *a*-axis YBCO films at 800 °C substrate temperature, under 100 mTorr of oxygen flow. The bilayer was then annealed in 50 Torr of oxygen for 1 h at 430 °C. Morphological features reminiscent of the flat and crystalline regions mentioned above were apparent also on the SRO-coated films. This is shown in Fig. 1(a), presenting an STM image of a 13 nm thick SRO layer overcoating a (100)YBCO film. The samples were transferred from the growth chamber in a dry atmosphere and introduced into our cryogenic STM after being exposed to ambient air for less than 10 min.  $R(T)$  curves of the SRO/(100)YBCO bilayers (for SRO layers thicker than 8 nm) clearly showed both the ferromagnetic transition at  $\sim 150$  K and the superconducting transition onset around 86–90 K as seen in Fig. 1(b), indi-

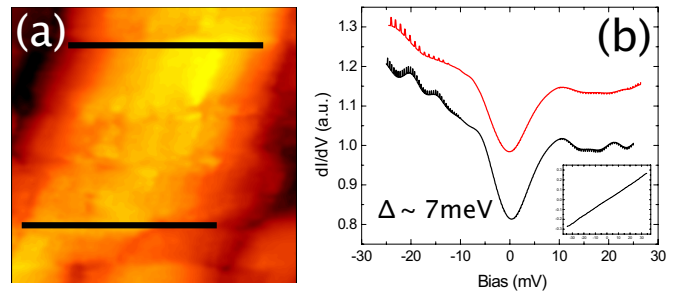


FIG. 2. (Color online) (a)  $300 \times 300 \text{ nm}^2$  2D STM image of a 9 nm thick SRO/YBCO bilayer on which an induced OP was detected along two elongated strips (marked). (b) Tunneling spectra taken, correspondingly, at the upper and lower strips marked in (a) (the upper curve is shifted vertically for clarity). Outside these gapped strips, only Ohmic  $I$ - $V$  curves were measured (inset).

cating that SRO layers at these thicknesses are still ferromagnetic but have no pronounced effect on the bulk superconductivity. [Zero resistance was obtained in Fig. 1(b) at 78 K.]

The STM data presented here were all acquired at 4.2 K using a (normal metal) Pt-Ir tip as seen in the inset to Fig. 1(b). The tunneling spectra were taken at specific well-defined locations correlated with the surface topography while momentarily disconnecting the feedback loop. Figure 2(a) presents a topographic image of a 9 nm thick (at least  $3 \xi_F$ ) SRO layer overcoating a (100)YBCO film. Within this region we observed two parallel strips, 200 nm apart (marked in black lines), along which gapped tunneling spectra were measured. Such strips will hereafter be referred to as “gapped strips.” The  $dI/dV$  vs  $V$  curves presented in Fig. 2(b) were taken correspondingly on the lower and upper gapped strips, both showing a pronounced minigap of  $\Delta \sim 7$  mV and a normalized (with respect to the normal conductance) zero bias conductance (ZBC) of  $\sim 0.8$ . We note that above  $T_c$ , no gaps were observed. FFLO-type PE theories<sup>5,6</sup> predict that the proximity induced OP should virtually vanish for this SRO thickness ( $\sim 3 \xi_F$ ) and consequently the ZBC should be 1. Indeed the area between the two marked strips featured exclusively Ohmic (gapless)  $I$ - $V$  curves [inset to Fig. 2(b)]. In most cases, the location of the strips had no correlation to detectable topographic features. This excludes the possibility that the induced gap in the DOS originates from a proximity to grain boundaries, cracks or other defects where the SRO thickness might be lower than the nominal value or that ferromagnetism could be locally suppressed. The distance between such gapped strips was in many cases [as in Fig. 2(a)] 200 nm, but larger separations were also observed, consistent with the domain structure of SRO reported in Ref. 30.

A more thorough mapping of the spatial evolution of the DOS in the vicinity of such a strip is presented in Fig. 3. Figure 3(b) depicts a  $260 \times 260 \text{ nm}^2$  topographic image of an 18 nm thick (at least  $6 \xi_F$ ) SRO layer overcoating a (100) YBCO film, where the center of a gapped strip is marked by the broken blue arrow. The spectra presented in Fig. 3(c) were acquired sequentially at equal steps along this strip. Clearly, the gap in the DOS is continuous and remarkably constant along the strip, over the whole length that was mea-

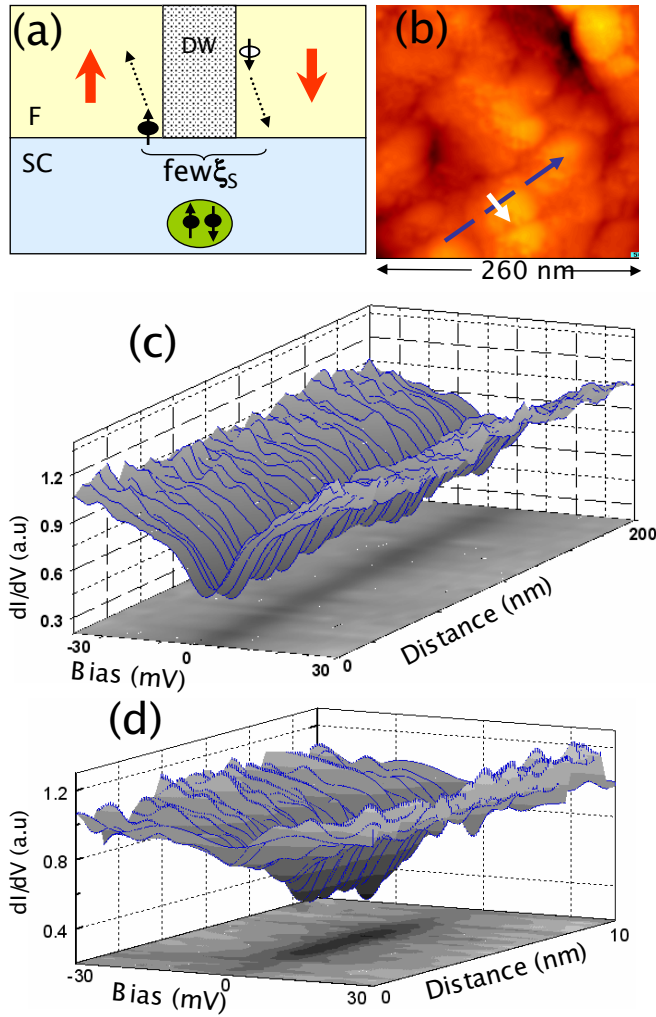


FIG. 3. (Color online) STM measurement demonstrating the spatial evolution of the DOS within a “gapped strip” in the SRO. (a) A schematic CARE diagram. (b)  $260 \times 260 \text{ nm}^2$  topographic image of a 18 nm thick SRO/(100)YBCO bilayer. (c) Tunneling spectra taken sequentially at fixed steps along the center of the gapped strip [marked by the blue arrow in (b)]. (d) Tunneling spectra acquired across the gapped strip [solid white arrow in (b)].

sured (about 200 nm). The tunneling spectra depicted in Fig. 3(d) were taken in a similar manner *across* the strip [solid white arrow in Fig. 3(b)] over a total length of 10 nm. Evidently, the width of the gapped area in the central region of this cross line is less than 8 nm, comparable to the width of the DWs in SRO ( $\sim 3 \text{ nm}$ ).<sup>30</sup> Within that narrow region, the gap is continuous and has a fixed width of 6.8 meV, while the ZBC shows small variations. Outside this central region, the gap decays abruptly over a length of a nm and the DOS becomes normal [see the projection onto the  $x$ - $y$  plane in Fig. 3(d)]. We note that the gap width and ZBC could vary from one strip to another on a specific film, but on average the gap structure weakened with increasing SRO layer thickness and gaps were only weakly observed on the 26 nm thick SRO film.

Interestingly, no gapped strips were detected on SRO films thinner than  $2\xi_F$ . Instead, the OP seemed to penetrate

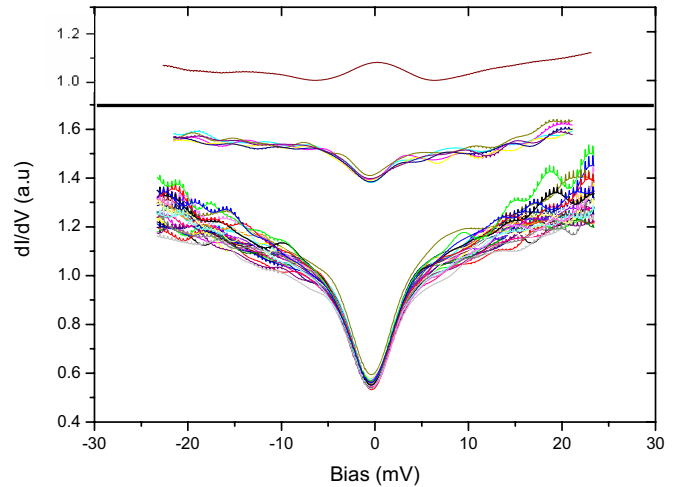


FIG. 4. (Color online) Lower panel: two sets of tunneling spectra taken at different areas ( $100 \times 100 \text{ nm}^2$  each) on a 6 nm thick SRO/(100)YBCO bilayer. Gap size and ZBC corresponding to the upper and lower sets are 3.8 mV, 0.85 and 4.5 mV, 0.56, respectively. Upper panel: a  $dI/dV$  curve showing a peak at zero bias, possibly manifesting a  $\pi$  state.

the  $F$  layer over large areas but in a nonuniform manner: for a given SRO layer thickness, gaps with a very wide distribution of ZBC (0.5 to 0.85) and gap width (3.8–7.5 mV) were observed. The lower panel of Fig. 4 depicts two sets of  $dI/dV$  curves acquired at two different areas ( $\sim 100 \times 100 \text{ nm}^2$  each) on a 6 nm thick SRO layer overcoating a (100)YBCO film. The wide distribution of the gap features cannot be solely due to SRO thickness variations. Possibly, in this low SRO thickness regime, ferromagnetism might be weakened in parts of the  $F$  layer and the domain structure may be lost. Indeed, the kink seen at 150 K in the  $R(T)$  curve of Fig. 1(b) could hardly be observed on these bilayers. The upper panel of Fig. 4 depicts a typical  $dI/dV$  curve obtained on a terrace adjacent to and slightly higher than the area where the small gap curves plotted just below it were measured. This curve shows a peak in the DOS at zero bias, the shape and size of which (compared to the curves plotted below it) are consistent with the FFLO OP oscillations picture and the formation of a  $\pi$  state.<sup>6,7</sup>

We suggest that the origin of the observed localized and long-range ( $\geq 10\xi_F$ ) penetration depth of the OP into the SRO layer is the CARE process, taking place along the DWs at the SRO/YBCO interface [see Fig. 3(a)]. Consequently, superconducting correlations can penetrate  $F$  quite efficiently in the vicinity of a DW. Naively speaking, Cooper pairs are injected into the  $F$  layer and can diffuse deeper inside only along a DW up to distances comparable to those of the PE in the  $S/N$  case.<sup>13</sup> Recall that the DW width is comparable to  $\xi_S$  (in the  $\text{CuO}_2$  planes) and much smaller than the phase coherence length ( $\sim \xi_N$ ) at 4.2 K, thus the conditions required for the local long range PE are satisfied, at least in the case where the DW is oriented along [001] direction. Such an orientation is consistent with the lattice parameter matching between YBCO and SRO and the well known domain structure in SRO.<sup>30</sup> The narrow width and the spacing of the elongated gapped strips in our measurements are indeed in

agreement with the known configuration and size of the DWs in SRO.<sup>30</sup> Our results support the recent magnetotransport evidence for CARE in YBCO/SRO/YBCO junctions with similar SRO layer thicknesses,<sup>28</sup> and corroborate the prediction that the total Andreev conductance of an  $S/F$  interface is proportional to the total length of the DWs crossing it.<sup>32</sup> The triplet pairing scenario for the long range PE is unlikely in our case since it would have resulted in a penetration of the OP *all over* the SRO layer. However, we cannot exclude the possibility that the long range PE may be due to the reduced spin polarization inside the DWs that may locally enhance the conventional AR.

We suggest that the CARE process may also account for the results reported by Gausepoh *et al.*<sup>17</sup> and Dömel *et al.*<sup>19</sup> In both cases, supercurrents were observed in YBCO/SRO/YBCO ramp junctions with 20 nm thick SRO barriers. In the former, nonuniformity in the supercurrent density over the area of the junctions was inferred from the magnetic response and related to the existence of favorable interface regions, less than 10 nm wide, through which the supercurrent flows. In the latter, the results were attributed to resonant

tunneling through localized states. Our data imply that the localized behavior in both cases may possibly be an effect of the existence of DWs in the SRO layer through which the superconducting electrodes couple. In the opposite case, where no DWs are present at an  $F/S$  interface, the “conventional” short range PE is expected to take place, as was recently demonstrated experimentally.<sup>33</sup>

In summary, we found a remarkably localized and long ranged PE in bilayers of SRO on (100)YBCO. For SRO layers thicker than  $\sim 3\xi_F$ , the OP penetrates the SRO to a distance larger than  $10\xi_F$  only along well defined localized lines which correlate with the underlying magnetic DW structure. This localized long range PE may thus be attributed to the CARE process taking place along the DWs of the SRO layers, although the contribution of reduced spin polarization at the DWs cannot be ruled out.

The authors are grateful to G. Deutscher and L. Klein, for useful discussions. This research was supported in part by the Israel Science Foundation, Center of Excellence program (Grant No. 1564/04).

\*Electronic address: milode@vms.huji.ac.il

<sup>1</sup>G. Deutscher and P. G. De Gennes, *Superconductivity* (Marcel Dekker, New York, 1969).

<sup>2</sup>R. J. Soulen *et al.*, *Science* **282**, 85 (1998).

<sup>3</sup>P. Fulde and R. A. Ferrell, *Phys. Rev.* **135**, A550 (1964).

<sup>4</sup>A. Larkin and Y. Ovchinnikov, *Sov. Phys. JETP* **20**, 762 (1965).

<sup>5</sup>E. A. Demler, G. B. Arnold, and M. R. Beasley, *Phys. Rev. B* **55**, 15174 (1997).

<sup>6</sup>A. Buzdin, *Rev. Mod. Phys.* **77**, 935 (2005).

<sup>7</sup>T. Kontos *et al.*, *Phys. Rev. Lett.* **86**, 304 (2001).

<sup>8</sup>V. V. Ryazanov *et al.*, *Phys. Rev. Lett.* **86**, 2427 (2001).

<sup>9</sup>M. Giroud *et al.*, *Phys. Rev. B* **58**, R11872 (1998).

<sup>10</sup>V. T. Petrashov *et al.*, *Phys. Rev. Lett.* **83**, 3281 (1999).

<sup>11</sup>Z. Faraii and M. Zareyan, *Phys. Rev. B* **69**, 014508 (2004).

<sup>12</sup>N. Stefanakis and R. Mélin, *J. Phys.: Condens. Matter* **15**, 3401 (2003).

<sup>13</sup>A. Sharoni *et al.*, *Phys. Rev. Lett.* **92**, 017003 (2004).

<sup>14</sup>I. Asulin *et al.*, *Phys. Rev. Lett.* **93**, 157001 (2004).

<sup>15</sup>M. Freamat and K. W. Ng, *Phys. Rev. B* **68**, 060507(R) (2003).

<sup>16</sup>V. Peña *et al.*, *Phys. Rev. B* **69**, 224502 (2004).

<sup>17</sup>S. C. Gausepohl *et al.*, *Appl. Phys. Lett.* **67**, 1313 (1995).

<sup>18</sup>L. Antognazza *et al.*, *Appl. Phys. Lett.* **63**, 1005 (1993).

<sup>19</sup>R. Dömel *et al.*, *Appl. Phys. Lett.* **67**, 1775 (1995).

<sup>20</sup>R. Dömel *et al.*, *Semicond. Sci. Technol.* **7**, 277 (1994).

<sup>21</sup>F. S. Bergeret, A. F. Volkov, and K. B. Efetov, *Phys. Rev. Lett.* **86**, 4096 (2001).

<sup>22</sup>A. F. Volkov, F. S. Bergeret, and K. B. Efetov, *Phys. Rev. Lett.* **90**, 117006 (2003).

<sup>23</sup>T. Heikkilä, Doctoral Dissertation, Helsinki University of Technology, 2002.

<sup>24</sup>J. M. Byers and M. E. Flatté, *Phys. Rev. Lett.* **74**, 306 (1995).

<sup>25</sup>G. Deutscher and D. Feinberg, *Appl. Phys. Lett.* **76**, 487 (2000).

<sup>26</sup>D. Beckmann, H. B. Weber, and H. v. Löhneysen, *Phys. Rev. Lett.* **93**, 197003 (2004).

<sup>27</sup>M. Giroud *et al.*, *Eur. Phys. J. B* **31**, 103 (2003).

<sup>28</sup>P. Aronov and G. Koren, *Phys. Rev. B* **72**, 184515 (2005).

<sup>29</sup>N. D. Zakharov *et al.*, *J. Mater. Res.* **14**, 4385 (1999).

<sup>30</sup>A. F. Marshall *et al.*, *J. Appl. Phys.* **85**, 4131 (1999).

<sup>31</sup>A. Sharoni *et al.*, *Europhys. Lett.* **62**, 883 (2003).

<sup>32</sup>N. M. Chitchev and I. S. Burmistrov, *Phys. Rev. B* **68**, 140501(R) (2003).

<sup>33</sup>J. Aumentado and V. Chandrasekhar, *Phys. Rev. B* **64**, 054505 (2001).